Evidence for the Proximity of the Extreme N-Terminus of the Neurokinin-2 (NK_2) Tachykinin Receptor to Cys^{167} in the Putative Fourth Transmembrane Helix†

Nirmala Bhogal,*,‡ Frank E. Blaney,§ Paul M. Ingley,‡ James Rees,‡ and John B. C. Findlay‡

School of Biochemistry and Molecular Biology, University of Leeds, Leeds LS2 9JT, U.K., and Computational, Analytical and Structural Sciences, GlaxoSmithKline NFSP (North), Harlow, Essex CM19 5AW, U.K.

Received August 18, 2003; Revised Manuscript Received November 26, 2003

ABSTRACT: Neurokinin-2 receptor (NK_2R) binding of [^{3}H]-SR48968, a piperidinyl antagonist, is inhibited by methanethiosulfonate ethylammonium (MTSEA) in a time- and concentration-dependent manner. By the systematic alanine replacement of putative loop and transmembrane region cysteine residues (Cys^4, Cys^{81}, Cys^{167}, Cys^{262}, Cys^{281}, Cys^{308}, and Cys^{309}), we have determined that MTSEA perturbs [^{3}H]-SR48968 binding by modifying Cys^{167} in transmembrane helix 4. Data were substantiated using glycine, serine, and threonine substitutions of Cys^{167}. MTSEA preferentially modifies cysteine residues that are in proximity to a negatively charged environment. Hence, aspartate and glutamate residues were systematically substituted with leucine or valine, respectively, and the inhibitory effects of MTSEA on [^{3}H]-SR48968 binding were reevaluated to determine those acidic residues close to the MTSEA binding crevice. Most significantly, substitution of Asp^5 in the receptor's extreme N-terminus abolished the effects of MTSEA on [^{3}H]-SR48968 binding. Therefore, our data would suggest close association of the extreme N-terminus with the extracellular surfaces of helices 4 and 3 in the NK_2R in forming a binding crevice for MTSEA. The inhibition of SR48968 binding appears to result from loss of the SR48968 binding conformation of Gln^{166} induced by MTSEA when it is coupled to Cys^{167}. Hence, it is proposed that there is mutually exclusive hydrogen bonding of SR48968 and MTSEA to Gln^{166}.

The mammalian neurokinin (NK) peptides, substance P (SP),[1] neurokinin A (NKA), and neurokinin B (NKB), are members of the tachykinin family. The peptides are distinguished by their common C-terminal Phe-X-Gly-Leu-Met-NH_2 motif. These neuropeptides fulfill their extensive nociceptive and cardiovascular roles by activating three widely distributed G-protein-coupled tachykinin receptors (NKRs). The receptors also share marked sequence similarities. Nevertheless, the mode of peptide, and indeed nonpeptide, ligand recognition varies between the three receptors subtypes (*1*). The aim of this work was to establish intramolecular contacts within the NK_2R to refine our current understanding of the nature of receptor−ligand recognition and receptor organization.

Early biochemical and protein engineering studies established that retinal and biogenic amines bind to receptor sites approximately 10 Å from the extracellular surface of the lipid bilayer (*2*, *3*). The recent crystal structure of rhodopsin substantiates the use of such approaches to determine the functional and organizational elements of GPCRs (*4*). More recently, Javitch et al. exploited a key interaction between catecholamines and the carboxylate side chain of a conserved aspartate residue in transmembrane helix 3 (TM3) (*5*) to map dopaminergic receptor binding sites and predict intrahelical periodicity. The substituted cysteine accessibility method (SCAM) was used to monitor sensitivity of antagonist binding to preexposure with MTSEA. The basis for utilizing MTSEA as a probe was its structural similarity to dopamine (*6*). The positively charged thiol reagent MTSEA was found to inhibit antagonist binding by occluding access to the TM3 aspartate residue. This approach has since been used to map binding determinants and transmembrane helical periodicity of other rhodopsin-like receptors (*7*).

Nonpeptide antagonists that target neuropeptide receptors may inhibit peptide agonist binding by their occupancy of overlapping binding crevices (*8*−*13*). However, it is more difficult to establish where these binding sites overlap. Very often there is no obvious common site of interaction. Instead, nonpeptide antagonists, upon interaction with predominantly transmembrane residues (*9*, *10*), may simply perturb more superficial interactions between the extracellular side of the helical bundle and the extracellular segments that are vital for peptide recognition (*8*, *11*, *12*). Despite some evidence for interplay between the extracellular regions and the TM bundle in peptide recognition (*13*), the organization of the extracellular regions is not well documented—due mainly

† This work was supported by an Industrial Fellowship from GlaxoSmithKline, U.K.

* To whom correspondence should be addressed. Tel (44) 113 2333178; fax (44) 113 2333167. E-mail: N.Bhogal@Leeds.ac.uk.

‡ University of Leeds.

§ GlaxoSmithKline NFSP (North).

[1] Abbreviations: SP, substance P; NKR, neurokinin receptor; NKA, neurokinin A; NKB, neurokinin B; GPCRs, G-protein-coupled receptors; [^{3}H]-SR48968, tritiated SR48968; SCAM, substituted cysteine accessibility method; SDM, site-directed mutagenesis; MTS, methane thiosulfonate; MTSEA, 2-aminoethyl MTS hydrochloride; MTSET, [2-(triethylammonium)ethyl] MTS bromide; MTSES, sodium (2-sulfonatoethyl) MTS; MMTS, methyl MTS; PMTS, propyl MTS; NEM, *N*-ethylmaleimide; MEM, methylmaleimide; PhEM, phenylmaleimide; CHO, Chinese hamster ovary; TM, transmembrane helix; ECL, extracellular loop; ABNR, adopted basis Newton Raphson.

10.1021/bi035475s CCC: $27.50
Published on Web 02/25/2004

to their highly flexible nature. Subsequently, any interactions between these regions and the TM bundle are notoriously difficult to model with any degree of reliability. The first step is to experimentally establish a number of contacts between the TM bundle and extracellular regions.

We have repeatedly observed that the inhibitory actions of MTS reagents are not restricted to those receptors that bind small catecholamine ligands (unpublished observations). The well defined binding requirements of MTS reagents make them suitable tools for indirectly determining receptor organization; for example, MTSEA, which contains a positively charged headgroup, is stabilized by negatively charged acidic residues. Furthermore, these small reagents are far more amenable to structural modeling than larger more flexible peptide ligands. Despite this, however, no publication to our knowledge has appeared on the computational simulation of these reagents.

Here we describe the use of thiol reagents in conjunction with site-directed mutagenesis (SDM) and molecular modeling to examine the intramolecular organization of the NK_2R by an adaptation of SCAM methodology. The contributions of native receptor cysteine and negatively charged residues to the inhibitory effects of MTSEA upon [^{3}H]-SR48968 binding were assessed to locate the site modified by MTSEA and to determine which charged side chains contribute to this receptor MTSEA binding site. Our data indicate that although none of the targeted sites are crucial binding determinants for [^{3}H]-SR48968, the [^{3}H]-SR48968 binding site lies in sufficient proximity to an MTSEA binding site within the NK_2R for the binding of [^{3}H]-SR48968 to be inhibited by MTSEA coupling to the receptor. MTSEA itself appears to modify Cys^{167} at the extracellular side of transmembrane helix 4. Somewhat suprisingly this interaction is, in turn, reliant on the presence of an aspartate residue, not in the extracellular loops but rather within the receptor's extreme N-terminus, thus placing the extreme N-terminus of the receptor near the extracellular sides of helices 3 and 4.

EXPERIMENTAL PROCEDURES

Materials. (±)-SR48968 and SR144190 were the kind gifts of Sanofi Recherché (*14*, *15*). [^{3}H]-SR48968 (specific activity 25 Ci/mmol, *16*) was purchased from NEN Dupont. The MTS (methane thiosulfonate) derivatives MTSEA (2-aminoethyl MTS hydrochloride), MTSET ([2-(triethylammonium)ethyl] MTS bromide), MTSES (sodium (2-sulfonatoethyl) MTS), MMTS (methyl MTS), and PMTS (propyl MTS) were supplied by Toronto Chemicals Inc. (Canada). *N*-ethylmaleimide (NEM), methylmaleimide (MEM), and phenylmaleimide (PhEM) were purchased from Sigma Chemical Co. General reagents were obtained from Sigma Chemical Co., Invitrogen Inc., or Boehringer Mannheim with the exception of the 96 well GF/B filter plates and manifold (Millipore).

Vectors and SDM. The human ileum NK_2R cDNA (from GlaxoSmithKlein (GSK), U.K.) was subcloned into the *Eco*RI site of mammalian expression vector pCDNA3.1 (Invitrogen, final construct denoted pCDNA3-NK_2R). SDM was performed using QuikChange mutagenesis (Stratagene), and mutations were confirmed by automated DNA sequencing (LARK Technologies Inc., U.K.).

CHO Cell Expression and Radioligand Binding Analysis. CHO cell monolayers were propagated to 60% confluence in a 37 °C humidified environment (5% CO_2) in complete medium (1:1 F12/HAM nutrient mixture containing Glutamax (Invitrogen) supplemented with 10% (v/v) fetal calf serum, 1 mM nonessential amino acid mixture, 100 μU/mL penicillin, and 100 μg/mL streptomycin). Thirty micrograms per milliliter wild-type or mutant pCDNA3-NK_2R DNAs were incubated with 10 μg/mL Lipofectamine (Invitrogen) in F12/HAM (15 min, RT). The transfection mixture was then diluted 10-fold with unsupplemented media and overlaid onto cell monolayers. Transfections were terminated after 5 h by adding 2 volumes of complete medium. Seventy-two hours post transfection, cells were plated into 24 well plates, and colonies were propagated in the presence of 1 mg/mL G418 from wells to suitable numbers for assay. Cells were harvested into binding buffer (20 mM HEPES, 400 μg/mL BSA, 200 μg/mL bacitracin in DMEM) for radioligand binding studies or PBS-Dulbecco's where preexposure to thiol reagents was required. Unless specified, $(1-3) \times 10^5$ cells were incubated with thiol reagents in 200 μL replicates for 5 min in 96 well GF/B filter plates prewetted with 0.3% (w/v) polyethyleneimine. Wells were then drained by filtration prior to binding analysis. The pharmacological profiles of the expressed receptors were assessed by Scatchard analysis using [^{3}H]-SR48968. Nonspecific binding was determined in the presence of 1000-fold excess SR144190. Data from scintillation counting were analyzed using Graph Prism v 3.0 (GraphPAD Software, San Diego, CA).

Computational Chemistry. The initial model of the TM domain of the NK_2R was constructed by homology with the published X-ray crystal structure of bovine rhodopsin (*4*). Alignments between this sequence and bovine rhodopsin were based on the "classical" motifs found in each TM region, namely, the asparagine in TM1, the aspartate in TM2, the "DRY" motif (ERY in rhodopsin) of TM3, the tryptophan in TM4, and the conserved prolines in TM5, TM6, and TM7. These alignments were used with the standard homology modeling tools in the Quanta program (Accelrys, La Jolla, CA), to construct the seven helical bundle domain.

The ECL regions were subsequently added using a procedure developed "in house", which makes use of a combined distance geometry sampling and molecular dynamics simulation (*17*). The model was then fully optimized (500 steps of Steepest Descent followed by 5000 steps of ABNR) with the CHARMm force field (Accelrys, La Jolla, CA) using helical distance constraints to maintain the backbone hydrogen bonds of the helix bundle.

The ligand molecule SR48968 and the MTSEA "patch" used in this study were initially constructed using the builder options within the Spartan program (Wavefunction Inc., Irvine, CA) and were further optimized at the semiempirical AM1 level using the Vamp program (Oxford Molecular Ltd., Oxford, U.K.). The resultant structures were then used to calculate ab initio charges for subsequent docking experiments. Natural atomic orbital charges were the ones of choice, and these were calculated with Spartan using a 3-21G* basis set. SR48968 was docked into the receptor model manually using a variety of low-energy conformations of the ligand. Adjustments of the protein side chains were made as was necessary, always ensuring that these side chains were only in allowed rotameric states. Once again,

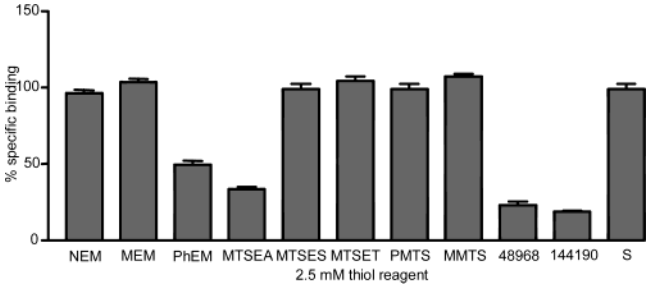

FIGURE 1: Thiol reagents that inhibit [^{3}H]-SR48968 binding to the NK_2R. Wild-type NK_2R expressing CHO cells were exposed to 2.5 mM final concentration of the indicated thiol reagent for 10 min prior to filtration and assessment of [^{3}H]-SR48968 binding (see Experimental Procedures for details). The ability of the receptor-specific unlabeled antagonists to inhibit specific binding (S) was also assessed at this stage using 1 nM SR48968 (48968) or SR144190 (144190). Data are expressed as percent specific binding of 0.5 nM [^{3}H]-SR48968 evident after thiol reagent exposure. Data shown are from five experiments performed in triplicate.

full optimizations of the receptor−ligand complexes were performed using CHARMm, the only constraints used being those that maintained the hydrogen bonding pattern of the helical bundle. This procedure thus allows full relaxation of both the ligand and the whole protein—something that is not possible with automated docking procedures. Several possible binding orientations were found, but only one concurred with experimental data (*8*, *18*, *19*). The cross-linking of MTSEA was modeled by using a patch residue technique within CHARMm. In this, the hydrogen of the cysteine thiol is removed, and a disulfide bond is formed with MTSEA. All new atom types, ab initio atomic charges, and internal coordinate definitions were then assigned to the thiolated cysteine for use in the CHARMm script. The high-temperature molecular dynamics simulations were performed at 1000 K using the Verlet method in CHARMm with the Shake algorithm applied to hydrogen atoms. After suitable heating and equilibration periods, the simulations were continued for a total period of 2 ns. The distance−time correlation diagrams were plotted directly from the CHARMm output using software written "in-house" at GSK.

RESULTS

MTSEA Inhibition of [^{3}H]-SR48968 Binding to the NK_2R. An initial assessment was conducted to determine the ability of various thiol reagents to modify the NK_2R in such a way that [^{3}H]-SR48968 binding was inhibited (Figure 1). All reagents were incubated with CHO cells expressing the wild-type NK_2R, and then binding of 0.5 nM [^{3}H]-SR48968 was assessed. Of the reagents assessed, only MTSEA inhibited [^{3}H]-SR48968 binding in a concentration- and time-dependent manner (see below). The bulkier positively charged MTS reagent, MTSET, exhibited no inhibitory activity. The negatively charged MTS reagent, MTSES, and the neutral PMTS and MMTS were also without effect. This is suggestive of a relatively small, negatively charged binding crevice for MTSEA.

The ability of PhEM to inhibit radioligand binding was observed repeatedly ($n = 7$). However, unlike MTSEA, PhEM seems to modify the NK_2R in a time- and concentration-independent manner. Hence, it is highly unlikely that PhEM modifies any site close to the [^{3}H]-SR48968 binding site. It is possible that by modifying lipid-facing sites, PhEM

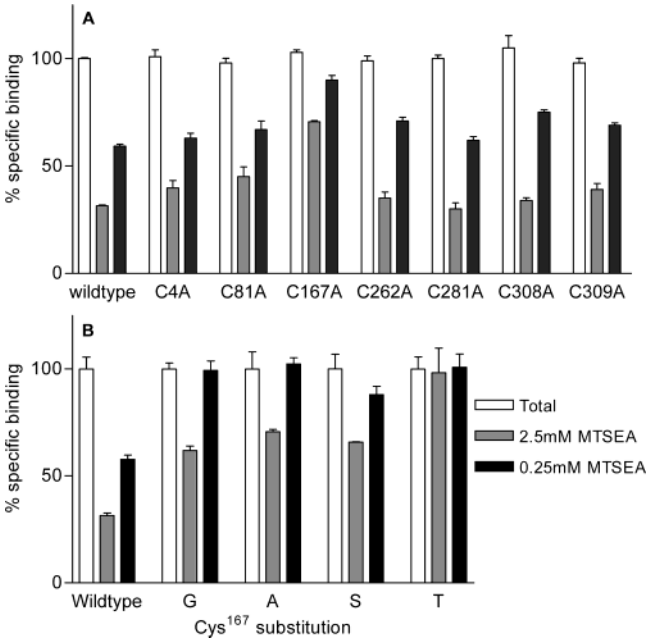

FIGURE 2: Identification of the site of MTSEA interaction. CHO cells expressing the wild-type and cysteine to alanine mutant receptors (A) or Cys^{167} mutants (B) were subjected to radioligand binding following a 5 min preexposure to MTSEA, essentially as described in the legend to Figure 1. Data shown are from six experiments performed in triplicate.

alters receptor conformation or the ability of receptors to adopt all possible high-affinity SR48968 binding conformations. Because assessment of such an interaction would prove difficult without a quantifiable parameter, further analysis was restricted to the analysis of MTSEA inhibition of [^{3}H]-SR48968 binding.

Identification of the Site of MTSEA Receptor Modification. Each of the transmembrane and extracellular region cysteine residues in the NK_2R was individually substituted with alanine to determine the site of MTSEA receptor modification (Figure 2A). In theory, removal of the cysteine side chain involved will abolish the inhibitory effects of MTSEA.

Table 1 shows the data from Scatchard analyses of the wild-type and alanine mutant receptors. The alanine mutants displayed (within 4-fold) wild-type K_d values for [^{3}H]-SR48968. B_{max} values (indicative of expression levels) were also comparable to those of the wild-type receptor. The greatest reduction in expression was 6-fold as seen for the Cys^{309}−Ala mutant.

Binding of [^{3}H]-SR48968 to Cys^{167}−Ala mutant receptors was substantially less (30−40%) sensitive to preexposure to 0.25 and 2.5 mM MTSEA than was the case for the wild-type receptor and the remaining alanine-substituted receptors. To further validate these observations, Cys^{167} was substituted with glycine, serine, and threonine. Glycine occupies the equivalent position within the human NK_1R subtype. Serine and threonine substitutions were made on the basis that they may be more readily accommodated within the aqueous environment. The results indicate that the glycine and serine mutants also exhibit (within 2-fold) wild-type K_d values for [^{3}H]-SR48968 (Table 1) and are expressed to wild-type levels but that MTSEA is once again less able to inhibit radioligand binding (Figure 2B). Most markedly, the threonine mutation abolished the inhibitory effects of MTSEA up to 20 mM. The fact that MTSEA cannot react with these mutant

Table 1: K_d and B_{max} Values for [^{3}H]-SR48968 Binding to Alanine-Substituted Mutants[a]

receptor	K_d (nM)	B_{max} (fmol/mg of cell protein)
wild-type	1.9 ± 0.3 (10)	1903 ± 402
Cys^4−Ala	4.2 ± 1 (3)	774 ± 451
Cys^{81}−Ala	0.5 ± 0.2 (3)	812 ± 208
Cys^{106}−Ala	NBD	NBD
Cys^{106}−Ala/Cys^{181}−Ala	NBD	NBD
Cys^{167}−Ala	0.9 ± 0.2 (6)	1235 ± 450
Cys^{167}−Gly	2.9 ± 0.2 (6)	2130 ± 367
Cys^{167}−Ser	0.9 ± 0.1 (4)	1560 ± 890
Cys^{167}−Thr	1.2 ± 0.2 (4)	1119 ± 607
Cys^{262}−Ala	1.4 ± 0.5 (3)	779 ± 163
Cys^{281}−Ala	6.2 ± 1.3 (3)	960 ± 189
Cys^{308}−Ala	1.7 ± 0.3 (3)	567 ± 98
Cys^{309}−Ala	1.8 ± 0.4 (3)	330 ± 132

[a] The affinity of [^{3}H]-SR48968 for expressed NK_2Rs was assessed by Scatchard analysis using 50 pM to 20 nM radioligand in the presence or absence of 1000-fold excess SR144190. Typically, 3×10^4 to 10^5 cells were used per assay well. BCA protein determinations were made (Sigma Chemical Co.). Data were subjected to nonlinear hyperbolic regression (one- and two-site fitting). All data conformed to the one binding site model. Means ± SEM are given with the number of triplicate experiments in parentheses. NBD indicates no specific binding detected within the concentration range of radioligand used.

Table 2: [^{3}H]-SR48968 Affinities for Receptors in Which the Negatively Charged Side Chains Were Removed[a]

receptor	K_d (nM)	B_{max} (fmol/mg of cell protein)
wild-type	1.9 ± 0.3 (10)	1903 ± 402
Asp^5−Val	3.4 ± 1.1 (3)	467 ± 321
Glu^9−Leu	4.5 ± 0.3 (3)	671 ± 118
Glu^{17}−Leu	6.7 ± 2.2 (2)	890 ± 437
Asp^{79}−Val	4.3 ± 0.6 (3)	1204 ± 309
Asp^{175}−Val	0.9 ± 0.1 (4)	984 ± 451
Glu^{187}−Leu	3.6 ± 0.7 (3)	1818 ± 479
Asp^{188}−Val	2.2 ± 0.6 (3)	994 ± 386
Glu^{277}−Leu	1.2 ± 0.5 (3)	1167 ± 317
Asp^{278}−Val	2.3 ± 1.1 (3)	345 ± 126
Glu^{187}−Leu/Asp^{188}−Val	8.2 ± 1.0 (3)	234 ± 119
Glu^{277}−Leu/Asp^{278}−Val	10.9 ± 3.3 (3)	329 ± 87

[a] No evidence is seen for any direct interaction of these residues with SR48968. Experimental details are the same as those described in Table 1. Means ± SEM are given with the number of triplicate experiments in parentheses.

receptors clearly suggests that the MTSEA when cross-linked to Cys^{167} occupies at least a small part of the [^{3}H]-SR48968 binding pocket

Contribution of Negatively Charged Side Chains to SR48968 and MTSEA Binding. The ligand SR48968 contains a positively charged center that is expected to form a salt bridge with an acidic residue in the binding site. At the same time, it is accepted that a negatively charged environment is required to stabilize the positively charged headgroup of MTSEA during binding. We therefore attempted to determine which, if any, of the aspartate and glutamate residues within the NK_2R would stabilize SR48968 binding or, alternatively, would interact with MTSEA when it is cross-linked to Cys^{167}. There are a number of extracellular and intramembranous candidates. These are Asp^5, Glu^9, and Glu^{17} in the N-terminal sequence, Asp^{79} in TM2, Asp^{175}, Glu^{187}, and Asp^{188} in ECL2, and Glu^{277} and Asp^{278} in ECL3. Glutamate and aspartate residues were substituted with leucine and valine, respectively. Again, Scatchard analysis indicates that none of these residues form part of the [^{3}H]-SR48968 binding site (Table 2). The largest observed changes in affinity were 4- and 5-fold approximately, which were seen for the double mutants Glu^{187}−Leu/Asp^{188}−Val and Glu^{277}−Leu/Asp^{278}−Val, respectively. Hence, because SR48968 has a protonated nitrogen, it is clear that none of the mutated acidic residues listed in Table 2 play a role in [^{3}H]-SR48968 binding because otherwise one would expect the binding affinity of one or more of these mutant receptors to be dramatically reduced.

The ability of MTSEA to perturb [^{3}H]-SR48968 binding was assessed (Figure 3). Glu^9−Leu, Glu^{17}−Leu, and Asp^{175}−Val exhibit quasi-wild-type MTSEA inhibition profiles. Glu^{187} and Asp^{188} in ECL2 and Glu^{277} and Asp^{278} in ECL3 may form part of an MTSEA binding domain as suggested by the reduced ability of 0.25 mM MTSEA to inhibit [^{3}H]-SR48968 binding to the double receptor mutants (see below). Similarly, [^{3}H]-SR48968 binding to Asp^{79}−Val receptors appears marginally less sensitive to MTSEA preexposure than is the case for the wild-type receptor. This may be an indirect consequence of the role of Asp^{79} in determining receptor activation (*18*).

However, by far the most significant change in MTSEA inhibition of [^{3}H]-SR48968 binding was observed for the extreme N-terminus mutant Asp^5−Val. This mutant demonstrated almost negligible reactivity with MTSEA even following prolonged exposure to MTSEA (Figure 4). Cys^{167}−Ala, consistent with the data presented thus far, exhibited slow and low-level MTSEA reactivity (Figure 4). Together these data suggest that there may be at least one additional thiolation site within the NK_2R accessible to MTSEA but that Asp^5 is crucial for MTSEA thiolation of Cys^{167}.

The SR48968 Binding Site. The presence of a basic protonated nitrogen in SR48968 is suggestive of a potential pairing acidic residue within its receptor binding site. With the exception of the deeply buried Asp^{79}, which is known to be involved in receptor function rather than in direct ligand binding (*18*), there are no acidic residues in the TM bundle. Our model also suggests that the ECL residues Glu^{187}, Asp^{188}, Glu^{277}, and Asp^{278} all sit on the exposed surface of their respective loops and cannot access the TM bundle. These in silico observations are substantiated by the data shown in Table 2: Single and paired mutations at these positions have little effect on the affinity of [^{3}H]-SR48968. Furthermore, SDM data has previously shown (*8*, *9*, *19*−*22*) the importance of certain other residues within the TM bundle and would, therefore, preclude the involvement of the above acidic residues.

This only leaves Asp^{175} as a possible salt bridge partner. Asp^{175} is oriented into the bundle in our model. Hence, a number of docking studies based on interaction of the basic nitrogen of SR48968 with this aspartate residue were performed. No solution could be found where the observed interactions from previous SDM studies could be accounted for. This is further supported by our data, which suggest that Asp^{175} is indeed not involved in SR48968 binding (Table 2). Our attention then turned to Lys^{180}, which is thought to play a role in the binding of some mixed NK_2R/NK_3R quinoline antagonists (*17*). Again no binding modes could be identified from docking, which supported the SDM data, although some very recent results with mutants of Lys^{180} suggest that this residue forms part of the SR48968 binding site (Bhogal et al.; unpublished observation). This lysine is believed to

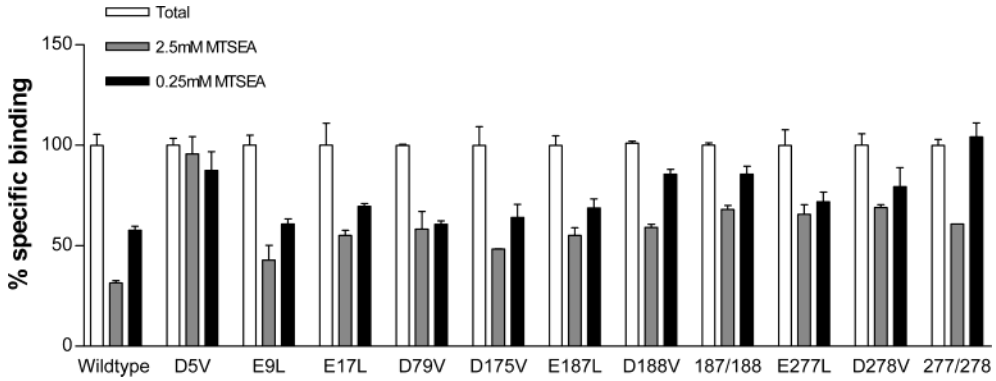

FIGURE 3: Assessment of the negatively charged microenvironment of MTSEA. Aspartate (D) and glutamate (E) residues were singularly or doubly substituted with valine (V) and leucine (L), respectively. The resultant mutant receptors were subjected to MTSEA inhibition assays as outlined in the legend to Figure 1. Data shown are from five experiments performed in triplicate.

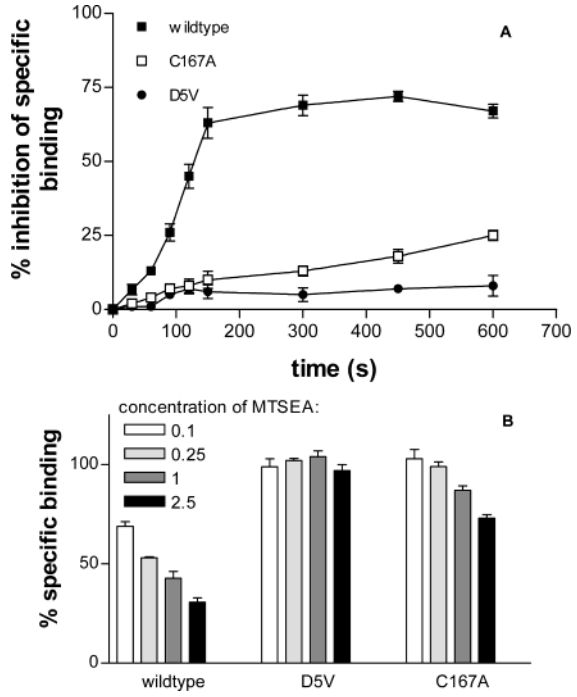

FIGURE 4: Modification of Cys^{167}−Ala and Asp^{5}−Val receptors by MTSEA. Receptor-expressing CHO cells were exposed to 2.5 mM MTSEA for between 30 and 300 s (A) or to varying concentrations (mM) of MTSEA for 5 min (B) prior to filtration and assessment of [^{3}H]-SR48968 binding (see legend to Figure 1). Data shown are from three (A) or four (B) experiments.

form a π-cation-type interaction with the dichlorophenyl ring (see below and Figure 5).

Our final docking studies focused on His^{198}. We have consistently shown (*8*, *19*) that mutation of this residue abolishes high-affinity binding of SR48968. The possibility that the protonated nitrogen of the ligand was hydrogen-bonding to the unprotonated imidazole nitrogen of His^{198} was, therefore, studied. The result (shown in Figure 5) is in perfect agreement with the SDM studies. The dichlorophenyl ring sits close to Lys^{180} with which it forms a π-cation interaction. In addition, SR48968 exhibits a coplanar π-stacking with Tyr^{266}, Tyr^{266} also forming an orthogonal aromatic interaction with the benzamide phenyl ring of the ligand: Tyr^{266}−Phe mutation has little effect on these interactions, as would be expected, whereas aliphatic substitutions at this position abolish ligand binding (*8*, *9*, *20*−*22*). The two amide carbonyls of the ligand are predicted to form hydrogen bonds with Gln^{166} and Tyr^{289}. Again, consistent with previous observations (*9*, *20*−*22*), mutations of these residues have been observed to adversely affect the binding of SR48968: Gln^{166}−Ile exhibits no detectable [^{125}I]-NKA or [^{3}H]-SR48968 binding. Tyr^{289}−Phe displays wild-type [^{125}I]-NKA binding, but SR48968 exhibits no discernible competition for [^{125}I]-NKA binding sites up to 10 μM, and [^{3}H]-SR48968 exhibits no detectable specific binding up to 20 nM.

Modeling the Environment of MTSEA. According to our model, although Cys^{167} is accessible to the thiolating group of MTSEA, the environment of MTSEA is dependent on the initial orientation of this receptor residue. All possible staggered conformations (180°, +60°, and −60°) of the χ_1 and χ_2 side chain angles and values of ±90° for the disulfide dihedral angle were used as starting points (18 in total) for the minimization of the MTSEA thiolated Cys^{167} protein model. Many of the resulting models could be immediately discarded because they oriented the thiolated side chain directly into the lipid bilayer. Three other broad conformational families were found. In the first, the positively charged amino headgroup of MTSEA formed a salt bridge with the carboxylate of Asp^{175}. As was seen above, however, Asp^{175} is not part of the binding site for SR48968 and does not reduce the extent of MTSEA inhibition of [^{3}H]-SR48968 binding. The second and more favored set of conformations showed the headgroup of MTSEA forming hydrogen bonds with the side chain carbonyls of Gln^{166} and Asn^{110} (Figure 6A). This conformation reorients the side chain of Gln^{166} from its SR48968 binding conformation (see above) and effectively breaks the hydrogen bond between Gln^{166} and SR48968. The final and most favored set of conformations has the MTSEA headgroup facing into the "exposed" top of the TM bundle between TM3 and TM4 (Figure 6B). For this conformation, there are no obvious stabilizing interactions with the MTSEA from the model, although it is entirely possible, given the experimental observation, that the receptor N-terminus folds over this area of the receptor.

The observed effect of the acid pairs Glu^{187}/Asp^{188} and Glu^{277}/Asp^{278} on MTSEA inhibition of SR48968 binding was examined by conformational sampling with high-temperature molecular dynamics. The starting points for the simulations were taken from the two main conformational families described above. After careful heating and equilibration at 1000 K, simulations were carried out for a period of 2 ns. The distances between the MTSEA nitrogen and various potential stabilizing residues were monitored throughout the

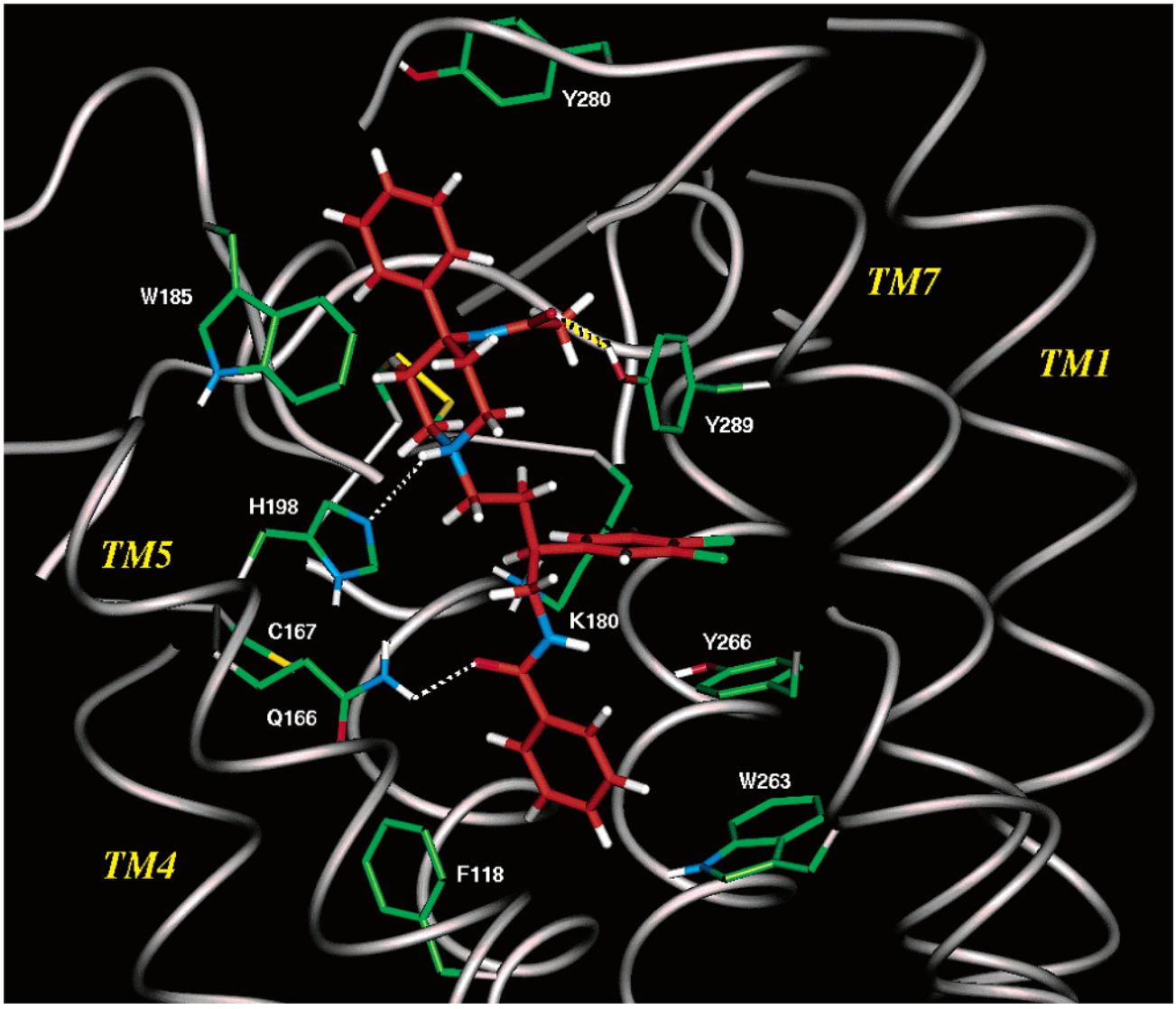

FIGURE 5: Proposed binding site for SR48968. The dotted lines represent strong hydrogen bonds, namely, Gln^{166} with an amide carbonyl, Tyr^{289} with the second amide carbonyl of SR48968 (orange) and His^{198} with the protonated nitrogen of SR48968. Tyr^{266} forms aromatic interactions with two of the phenyl rings of SR48968. Lys^{180} exhibits a π-cation interaction with the dichlorophenyl ring of SR48968.

trajectory. The results are shown (A) starting from the MTSEA headgroup hydrogen bonded to Gln^{166} and Asn^{110} and (B) starting with the headgroup exposed between TM3 and TM4 in Figure 7. Even at 1000 K, it is clear from Figure 7A that the protonated headgroup never really moves far from Gln^{166} and Asn^{110}. During the trajectory, it never approaches the carboxylates of Asp^{175}, Glu^{187}, Asp^{188}, Glu^{277}, or Asp^{278}. Nor does it ever approach other residues in the binding site such as His^{198}. From Figure 7B, it can be seen that the MTSEA headgroup makes occasional transitory contacts with Gln^{166} but not with Asn^{110}. It does not come within reach of the acid pairs Glu^{187}/Asp^{188} and Glu^{277}/Asp^{278}. Throughout most of the trajectory the MTSEA headgroup does form a salt bridge with Asp^{175}, although it can move away significant distances (up to 12 Å) from this aspartate. This does not preclude the interaction with further extracellular residues that are not included in the model. Hence, as a final experiment, the MTSEA patch was used to thiolate the ECL3 cysteine, Cys^{281}, that according to our model is exposed on the extracellular surface. A molecular dynamics simulation was carried out (using the same protocol as before), and the trajectory distances were monitored (Figure 7C). Significant salt bridge formation was observed between the MTSEA headgroup and the ECL3 residues Glu^{277} and Asp^{278}. No interactions, however, were seen with the ECL2 acidic residues Asp^{175}, Glu^{187}, and Asp^{188} or with the TM residues Asn^{110}, Gln^{166}, and His^{198}.

DISCUSSION

Here we report the use of chemical modification and protein engineering to identify the binding environment of MTSEA and gain an insight into the structural organization of the tachykinin NK_2R. The initial aim was to identify the thiolation site(s) of MTSEA and then to examine those acidic receptor side chains that contribute to the MTSEA binding site. Data generated using a combination of SDM, thiolation, and receptor characterization studies were subjected to molecular modeling.

Receptor-Bound MTSEA Occludes Access to the SR48968 Binding Site. Cys^{167}, which resides close to the extracellular side of TM4, was found to be a key site of thiol interaction with MTSEA (Figures 1 and 2). It is thiolation of this

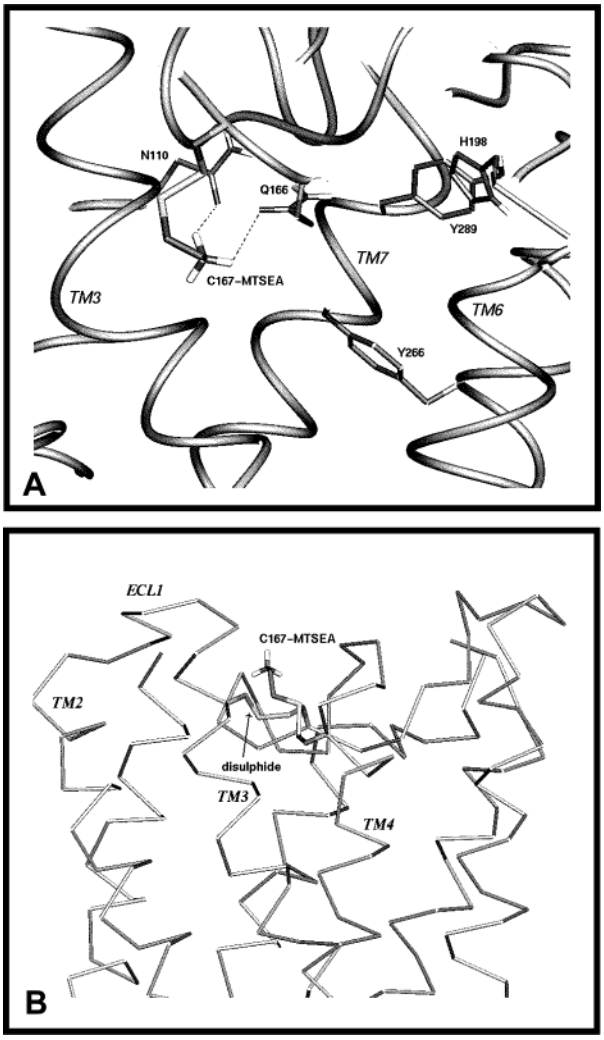

FIGURE 6: Alternative conformations of MTSEA cross-linked to Cys^{167}: (A) the ammonium headgroup of MTSEA interacts with Asn^{110} and Gln^{166}, breaking the interaction of the latter residue with SR48968; (B) the headgroup extends to the exterior of the TM bundle between TM3 and TM4. In conformation B, MTSEA is believed to interact with Asp^5.

cysteine by MTSEA that appears to inhibit the binding of the small receptor selective antagonist [^{3}H]-SR48968 since the mutant receptors Cys^{167}−Ala, Cys^{167}−Gly, Cys^{167}−Ser, and Cys^{167}−Thr exhibit reduced susceptibility of [^{3}H]-SR48968 binding to MTSEA pretreatment; the effects of MTSEA on [^{3}H]-SR48968 binding are not totally abolished by the removal of this cysteine. This may be indicative of MTSEA reactivity with some other cysteine residue(s) that are (a) more remote from the [^{3}H]-SR48968 binding site, (b) less accessible, or (c) only transiently exposed to the aqueous environment but thiolation of which has some influence on [^{3}H]-SR48968 binding.

Figures 8 and 9 demonstrate the putative disposition of cysteine residues within the NK_2R. Since MTSEA modifies thiol groups accessible from the extracellular side of the membrane 30 times faster than those accessible from the intracellular side of the plasma membrane (*23*) and since the intracellular environment is reducing, the least likely candidates are Cys^{324}, Cys^{325}, and Cys^{351} in the receptor C-terminus. Similarly, Cys^{308} and Cys^{309} near the intracellular side of TM7 are presumably not accessible owing partly to their location and partly to the overall aromatic nature of the pocket in which they reside.

Cys^{106} and Cys^{181} are involved in a well-documented disulfide bond implicated in receptor trafficking, folding, and function (*24*−*26*). Consistent with this, mutants lacking cysteines in these positions exhibit no discernible [^{3}H]-SR48968 binding (Table 1). Elimination of these residues from our enquiry was absolutely necessary since, should they not participate in disulfide bond interaction, they occupy positions highly susceptible to MTSEA thiolation.

This leaves four potential residues as candidates for secondary modification by MTSEA: Cys^4, Cys^{81}, Cys^{262}, and Cys^{281}. Our SDM data (Table 1) suggest that none of these residues are close to the SR48968 binding site. According to our 3D model, Cys^{81} packs against TM3 and Cys^{262} faces TM7 thus placing these transmembrane cysteines in environments less accessible to MTSEA. Both these residues are quite remote from the proposed SR48968 binding site. Cys^4 and Cys^{281} in the exposed extracellular domains are more likely to be the sites of secondary modification. Both these residues demonstrate either linear or spatial proximity to one or more negatively charged side chains, and given the likelihood that there is at least some degree of receptor resonance, MTSEA modification of any one or more of these sites cannot be excluded. This is clearly demonstrated by the molecular dynamics simulation of MTSEA linked Cys^{281} where the headgroup is stabilized by interactions with Glu^{277} and Asp^{278} (Figure 7C). However, both SDM data (Table 1) and docking studies (Figure 5) indicate neither Cys^4 nor Cys^{281} form part of the SR48968 binding site.

Consistent with our previous observations (*19*), the data presented indicate that Cys^{167} does not form part of the [^{3}H]-SR48968 binding site per se (Table 1). In fact, our model suggests that SR48968 never lies closer than 8 Å away from Cys^{167}. Instead it is proposed that [^{3}H]-SR48968 interacts with a binding site that in the correct conformation can be affected by the MTSEA thiolation of Cys^{167}. SDM studies have shown that SR48968 binding appears to involve interactions with His^{198} and Tyr^{266} (*8*, *9*, *19*, *24*−*26*). There is also evidence of a hydrogen bond interaction between Tyr^{289} in TM7 and SR48968 since the replacement of Tyr^{289} with phenylalanine abolishes high-affinity SR48968 binding (*26*). The singular substitutions of Gln^{166} with alanine or valine or of Thr^{171} with alanine reduce the affinity of SR48968 by approximately 5-fold (*9*, *20*). Our model suggests that the latter mutation causes a conformational change in ECL2, but all the other mutations above are clearly accounted for. Furthermore, as shown above, mutations of the negatively charged Asp^{175}, Glu^{187}, and Asp^{188}, and indeed the remaining residues in the distal portion of ECL2, have no effect on SR48968 binding (Table 2), again in keeping with our 3D model.

The MTSEA Microenvironment. The inability of most maleimides, and indeed the remaining MTS derivatives, to inhibit [^{3}H]-SR48968 binding provides additional clues as to the nature of the binding environment of MTSEA. The data are suggestive of a tightly constrained negatively charged MTSEA binding crevice—particularly given the lack of inhibitory action of the similarly charged but bulkier MTSET. Hence, the microenvironment of MTSEA was assessed further by aliphatic substitution of negatively charged residues within the putative extracellular and intramembranous regions (Figure 3).

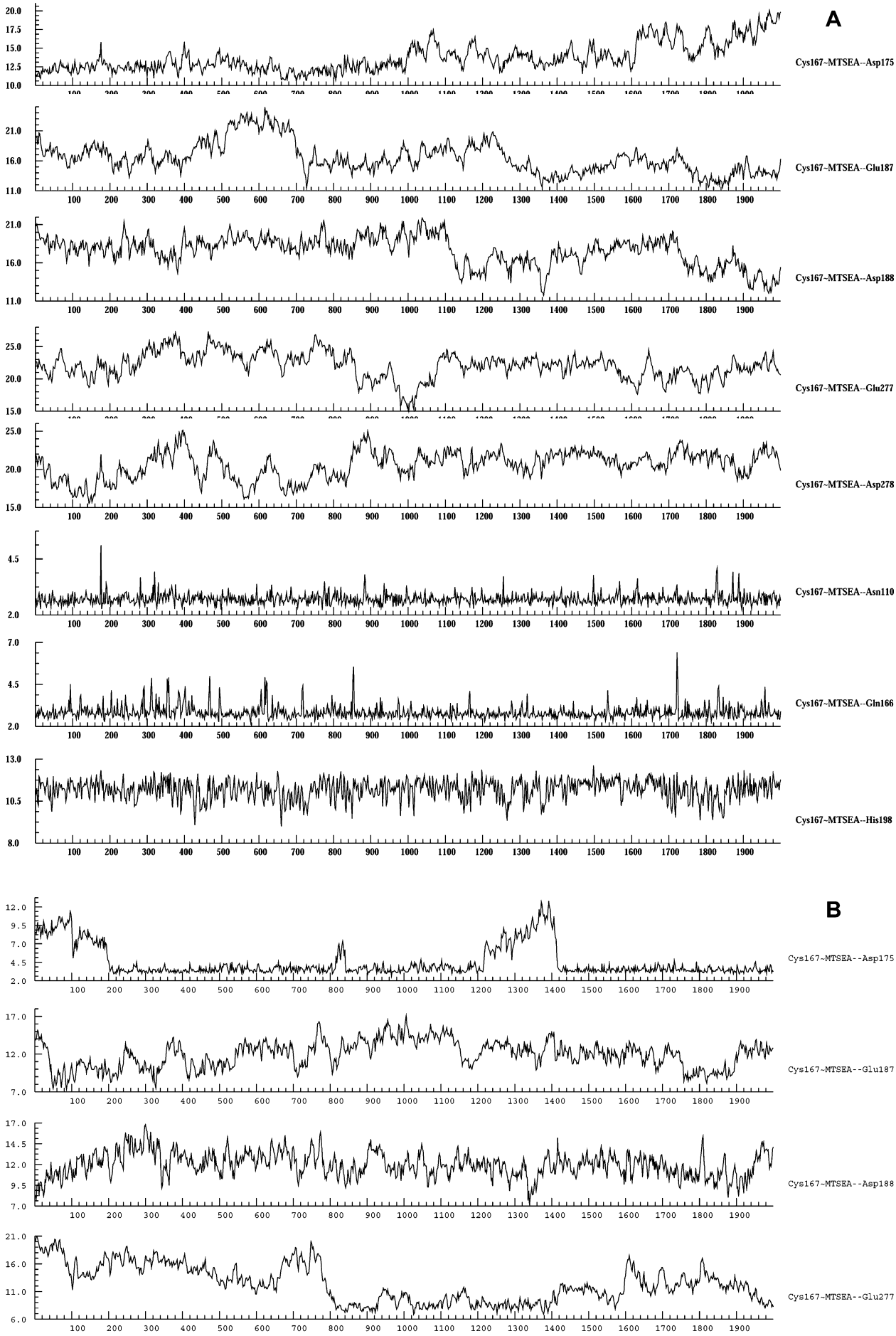
A
Cys167~MTSEA--Asp175
Cys167~MTSEA--Glu187
Cys167~MTSEA--Asp188
Cys167~MTSEA--Glu277
Cys167~MTSEA--Asp278
Cys167~MTSEA--Asn110
Cys167~MTSEA--Gln166
Cys167~MTSEA--His198
B
Cys167~MTSEA--Asp175
Cys167~MTSEA--Glu187
Cys167~MTSEA--Asp188
Cys167~MTSEA--Glu277

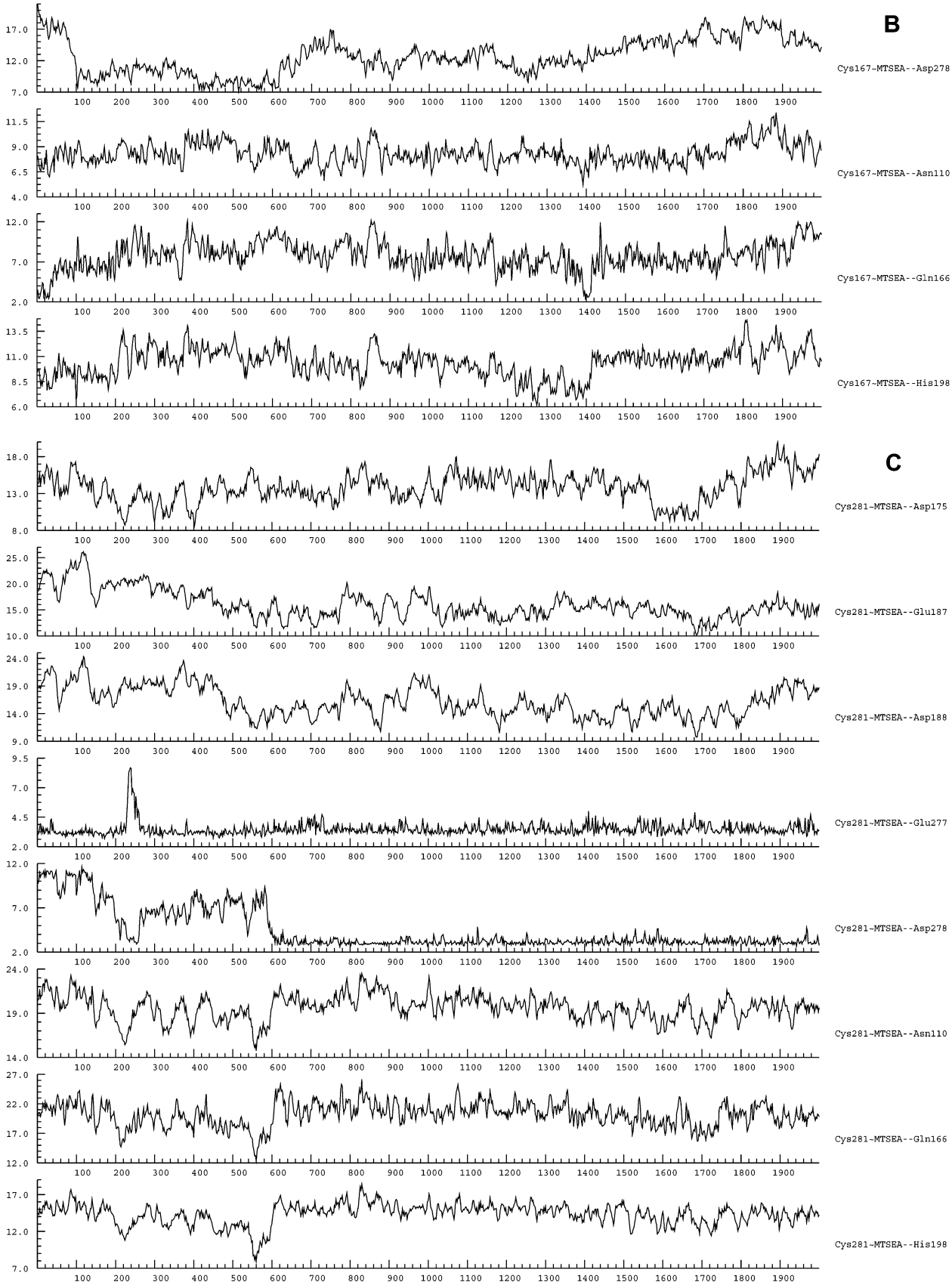

FIGURE 7: Distance correlations of the MTSEA headgroup with various residues. Molecular dynamics trajectories are shown. In each graph, the *x*-axis is the time interval in picoseconds and the *y*-axis is the relevant distance in angstroms. The residue being monitored is given in the legend on the right of each graph. Expected interaction distances would be in the range of 2.0−3.5 Å. Part A shows the trajectory for MTSEA cross-linked to Cys^{167} starting in the conformation as in Figure 6A. Part B shows the same trajectory as part A but starting from the conformation Figure 6B. Part C shows the trajectory for MTSEA cross-linked to Cys^{281}.

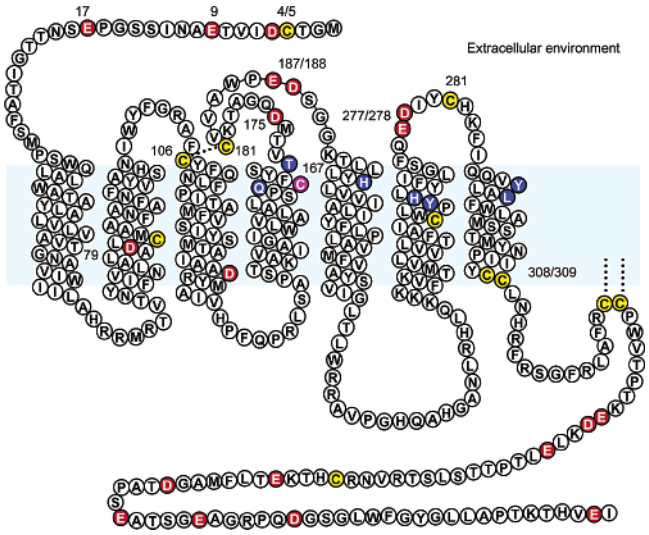

FIGURE 8: Serpentine representation of the NK_2R. The disposition of the native cysteine (yellow) and negatively charged residues (red) are shown alongside those residues that are known to form part of the SR48968 binding site (blue). Cys^{167} (purple), the putative disulfide bond between Cys^{106} and Cys^{181} (dotted line) and potential palmitoylation sites (Cys^{324} and Cys^{325}) are also indicated.

Replacement of Asp^5 with valine effectively abolishes the ability of MTSEA to inhibit [^{3}H]-SR48968 binding. This suggests that Asp^5 lies within 6−7 Å of Cys^{167} for it to stabilize the MTSEA headgroup (Figure 10). This effect was not observed when either of the two remaining negative charges in the N-terminus was removed emphasizing the specific nature of the role of Asp^5. According to our model, Asp^5 cannot project into the SR48968 binding site. Therefore, it is likely that SR48968 lies close to the headgroup of MTSEA as it couples to Cys^{167}. Indeed, given the specific requirement of a nearby negatively charged environment for MTSEA coupling, it is likely that Asp^5 is the driving force for the coupling reaction itself. Figure 4 clearly illustrates this point: While mutants lacking a cysteine at position 167 exhibit some, if dramatically reduced, susceptibility to MTSEA thiolation, the mutant that lacks an aspartate at position 5 displays no increase in MTSEA susceptibility with time or concentration. This can only suggest that Cys^{167} is not thiolated at all if Asp^5 is substituted with alanine.

We have indicated that the adjacent Cys^4 does not reside close to the [^{3}H]-SR48968 binding site (see above). Nor does the thiol group of this cysteine appear to orient toward the headgroup of MTSEA (Figure 7). This suggests that when Asp^5 is in the locality of Cys^{167}, Cys^4 projects away from the top of TM4 and away from the SR48968 binding site. We can conclude from the results that both Asp^5 and Cys^{167} are necessary for effective blockade of SR48968 binding. The molecular dynamics simulation (Figure 7A) would suggest that this must occur by stabilizing the headgroup of MTSEA coupled to Cys^{167} as it extends out of the TM bundle, a conformation that is remote from the SR48968 binding site.

The molecular dynamics simulations with MTSEA linked Cys^{167} (Figure 7) show that several conformational states are possible. One of these involves stabilization by hydrogen bonding with Gln^{166} (Figure 7B). In so doing, this is predicted to break hydrogen bonding between Gln^{166} and SR48968 and, hence, should lower the affinity of the ligand. This is particularly compelling since the mutation Gln^{166}−Ile adversely affects SR48968 binding (unpublished data). The most favored conformational state of the MTSEA, however,

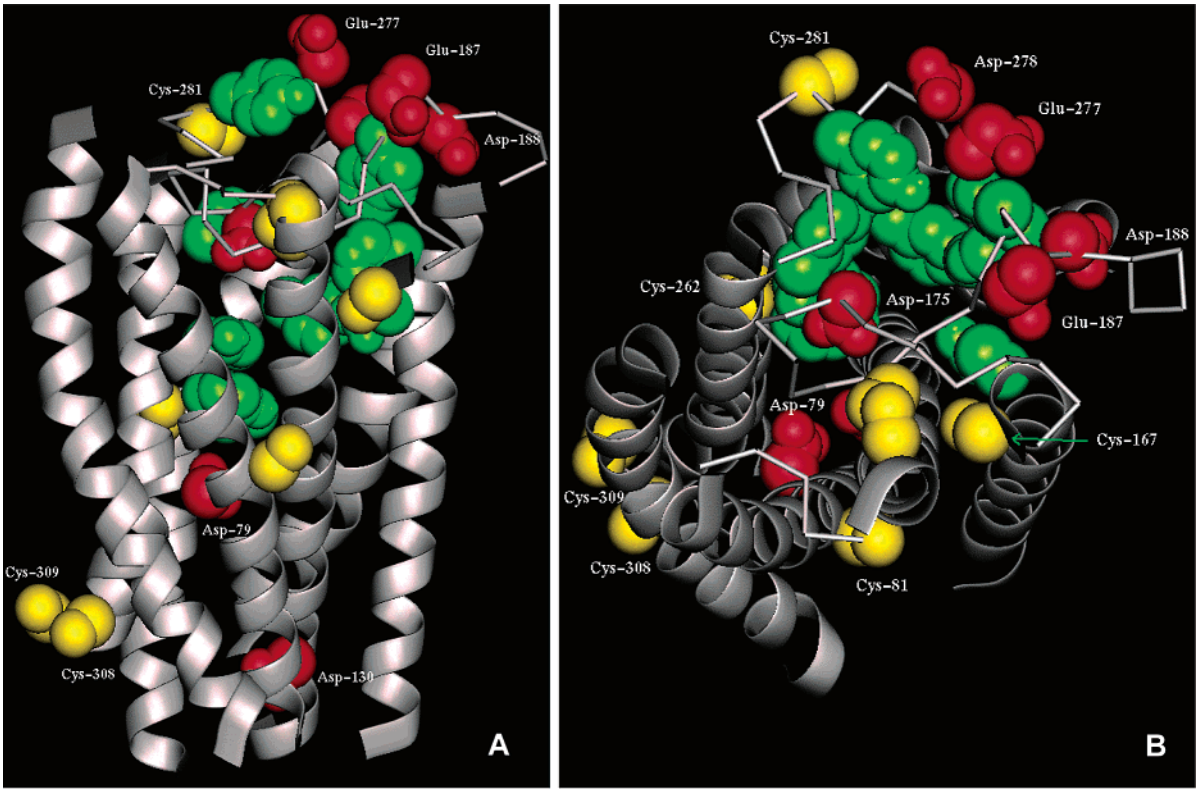

FIGURE 9: 3D model of the NK_2R. Orthogonal views of the NK_2R showing (A) a side view transversing the membrane and (B) a view in the plane of the membrane as seen from the extracellular environment. Positions of cysteine (yellow), aspartate and glutamate (red), and SR48968 binding residues (green) are shown.

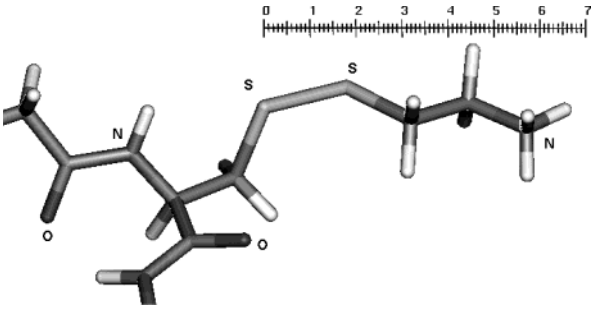

FIGURE 10: A cysteine residue coupled to MTSEA. The ruler shows that the distance between the cysteine sulfur and the ammonium headgroup is 6.5 Å.

involves the headgroup sitting on the extracellular side between TM3 and TM4 as described above (Figure 7A). This interaction may be partially stabilized by a salt bridge formation with Asp^{175}. Nevertheless, the reduced susceptibility of SR48968 binding to MTSEA preexposure displayed by the Asp^5−Val mutant would suggest that Asp^5 forms the main counterion for MTSEA. It is quite likely, in fact, that the presence of Asp^5 is necessary for the coupling reaction to occur. Once the reaction does take place however, the simulations show that the MTSEA ammonium headgroup can exist in equilibrium between two environments, one of which is stabilized by interaction with Asp^5 and the other in which hydrogen bonding with Gln^{166} prevents Gln^{166} hydrogen bonding to SR48968.

The contributions of negatively charged residues in ECL2 and ECL3 are less obvious. Changes in sensitivity of [^{3}H]-SR48968 binding to MTSEA preexposure and 4−5-fold changes in [^{3}H]-SR48968 affinity were only observed upon the concurrent removal of both Glu^{187} and Asp^{188} in ECL2 or of Glu^{277} and Asp^{278} in ECL3 (Table 2). The dynamics simulations certainly suggest that none of these four residues can lie in close proximity to the MTSEA headgroup when cross-linked to Cys^{167} (Figure 7). Nevertheless, it seems that several of the negatively charged residues on the extracellular side of TMs 4−7 may also form part of a putative second MTSEA binding crevice that is distant from the SR48968 binding site and, therefore, is not identifiable from our study. From our model, it would appear that Glu^{277} and Asp^{278} could certainly stabilize MTSEA when it is cross-linked to Cys^{281}. In contrast, the trajectory (Figure 7C) shows that Glu^{187} and Asp^{188} do not stabilize MTSEA cross-linked to either Cys^{167} or Cys^{281}. It is possible, therefore, that they may be stabilizing a further thiolation site. More probably, although these four residues do not contribute directly to the SR48968 binding site, they do form a large attractive negatively charged area across the putative ligand "entry pocket". Neutralization or removal of these residues would therefore be expected, as is observed, to have some effect on ability of MTSEA to inhibit SR48968 binding (Figure 3).

Consistent with previous observations, Asp^{79} neither forms part of the direct SR48968 binding site nor lies close to it. This residue appears to pack against and is functionally coupled to Asn^{303} in TM7 (*18*).

Molecular Organization of the Extracellular Receptor Domains. Our observations are in agreement with the observed crystal structure of bovine rhodopsin in that they indicate that the extracellular segments of the NK_2R, as in rhodopsin, adopt a level of organization whereby the receptor N-terminus overlays the remaining extracellular regions and potentially make extensive intramolecular contacts (*4*, *27*). Another example of this is found in the angiotensin II receptor where it is evident that a disulfide bond in addition to that conserved throughout family A receptors is necessary to maintain the recognition site for agonists but not peptidic antagonists (*28*). This second disulfide bond is formed between cysteine residues in the extreme N-terminus and ECL3. In the NK_2R, however, given the probable proximity between Cys^{167} and Asp^5, it is highly unlikely that the adjacent Cys^4 can occupy a position amenable to a disulfide bond with Cys^{281}. This is also in keeping with the lack of proximity between Cys^4 and the [^{3}H]-SR48968 binding site.

CONCLUSIONS

In conclusion, by systematic substitution of accessible cysteine, aspartate, and glutamate residues, we have identified the NK_2R binding environment of the thiol-modifying reagent MTSEA. It seems that MTSEA reacts primarily with Cys^{167} near the extracellular side of TM4. Our data suggest that Asp^5 lies in close proximity to the thiolated Cys^{167} and is largely responsible for providing the requisite negatively charged environment both for the reaction to occur, and for stabilization of the end product.

Owing to the inhibitory effects of MTSEA preexposure on [^{3}H]-SR48968 binding, it is proposed, in line with existing data, that when MTSEA is linked to Cys^{167} it adopts one conformation where the ammonium headgroup lies in close spatial proximity to the [^{3}H]-SR48968 binding site. However, Cys^{167} itself does not form any part of the [^{3}H]-SR48968 binding site.

Potentially, once thiolation has occurred, the ammonium headgroup of MTSEA, like SR48968, can make interactions with Gln^{166} where hydrogen bonding to this residue is mutually exclusive. Mutation of Asp^5, however, is likely to abolish the interaction of MTSEA with Cys^{167} because of the lack of a nearby negatively charged environment. In this case, hydrogen bonding of SR48968 to Gln^{166} will not be affected. This is supported by SDM data for Gln^{166}.

In summary, we have utilized a combination of in silico, protein engineering, and protein chemical analyses to address receptor organization. We have docked both the receptor specific antagonist SR48968 and MTSEA—a small thiolating reagent—into the 3D model of the NK_2R and examined the possible conformations of each ligand in accordance with experimental data to determine the probable organization of the extracellular N-terminus in relation to the TM bundle. Molecular dynamics simulations have shown that two main conformations of MTSEA coupled Cys^{167} are possible, one of which is probably necessary for the thiolation to occur (Asp^5) and the second of which—despite the apparent distance between SR48968 and Cys^{167}—is responsible for the adverse effect on SR48968 binding. This loss of binding is believed to result from alteration of the conformation of Gln^{166}, which in the wild-type receptor forms part of the SR48968 binding site.

Our data and subsequent analyses provide evidence of contacts between the extracellular and transmembrane regions of the NK_2R and provide some information toward the eventual modeling of contacts between these regions. Perhaps more importantly, these studies can be extrapolated to other GPCRs.

ACKNOWLEDGMENT

We thank Miss Abigail Melton and Mr. Adam Lockhart for their assistance.

REFERENCES

1. Maggi, C. A., and Schwartz, T. W. (1997) The dual nature of tachykinin NK_1 receptor, *Trends Pharmacol. Sci. 18*, 351−355.
2. Wang, H. Y., McDowell, H., and Hargrave, P. A. (1980) The attachment of 11-*cis*-retinal in bovine rhodopsin, *Biochemistry 19*, 5111−5117.
3. Dixon, R. A. F., Sigal, I. S., Rands, E., Register, R. B., Candelore, M. R., Blake, A. D., and Strader, C. D. (1987) Ligand binding to the β-adrenergic receptor involves its rhodopsin-like core, *Nature (London) 326*, 73−77.
4. Palczewski, K., Kaumasaka, T., Hori, T., Behnke, C. A., Motishima, H., Fox, B. A., Le Trong, I., Teller, D. C., Okada, T., Stenkamp, R. E., Yamamoto, M., and Miyano, M. (2000) Crystal structure of rhodopsin: A G protein-coupled receptor, *Science 289*, 739−745.
5. Strader, C. D., Sigal, I. S., Candelore, M. R., Rands, E., Hill, W. S., and Dixon, R. A. F. (1988) Conserved aspartic acid residues 79 and 113 of the β-adrenergic receptor have different roles in receptor function, *J. Biol. Chem. 263*, 10267−10271.
6. Javitch, J. A., Ballesteros, J. A., Weinstein, H., and Chen, J. (1998) A cluster of aromatic residues in the sixth membrane-spanning segment of the dopamine D2 receptor is accessible in the binding-site crevice, *Biochemistry 37*, 998−1006.
7. Xu, W., Chen, C., Huang, P., Li, J., de Riel, K., Javitch, J. A., and Lui-Chen, L.-Y. (2000) The conserved cysteine 7.38 residue is differentially accessible in the binding-site crevices of the μ, δ, and κ opioid receptors, *Biochemistry 39*, 13904−13915.
8. Labrou, N. E., Bhogal, N., Hurrell, C. R., and Findlay, J. B. C. (2001) Interaction of Met^{297} in the seventh transmembrane segment of the tachykinin NK_2 receptor with neurokinin A, *J. Biol. Chem. 276*, 37944−37949.
9. Huang, R.-R. C., Vicario, P. P., Strader, C. D., and Fong, T. M. (1995) Identification of residues involved in ligand binding to the neurokinin-2 receptor, *Biochemistry 34*, 10048−10055.
10. Gether, U., Emonds-Alt, X., Breliere, J.-C., Fujii, T., Hagiwara, D., Pradier, L., Garret, C., Johansen, T. E., and Schwartz, T. W. (1994) Evidence for a common molecular mode of action for chemically distinct nonpeptide antagonists at the neurokinin-1 (substance P) receptor, *Mol. Pharmacol. 45*, 500−508.
11. Turcatti, G., Zoffmann, S., Lowe, J. A., III, Drozda, S. E., Chassaing, G., Schwartz, T. W., and Chollet, A. (1997) Characterization of non-peptide antagonist and peptide agonist binding sites of the NK1 receptor with fluorescent ligands, *J. Biol. Chem. 272*, 21167−21175.
12. Fong, T. M., Yu, H., Huang, R.-R. C., and Strader, C. D. (1992) The extracellular domain of the neurokinin-1 receptor is required for high affinity binding of peptides, *Biochemistry 31*, 11816−11811.
13. Schambye, H. T., Hjorth, S. A., Bergsma, D. J., Sathe, G. and Schwartz, T. W. (1994) Differentiation between binding sites for angiotensin II and nonpeptide antagonists on the angiotensin II type 1 receptors, *Proc. Natl. Acad. Sci. U.S.A. 91*, 7046−7050.
14. Emonds-Alt, X., Advenier, C., Croci, T., Manara, L., Neliat, G., Poncelet, M., Proietto, V., Santucci, V., Soubrie, P., Van Broeck, D., Vilain, P., Le Fur, G., and Breliere, J. C. (1993) SR48968, a neurokinin A (NK_2) receptor antagonist, *Regul. Pept. 46*, 31−36.
15. Emonds-Alt, X., Advenier, C., Cognon, C., Croci, T., Daoui, S., Ducoux, J. P., Landi, M., Naline, E., Neliat, G., Poncelet, M., Proletto, V., VanBroeck, D., Vilain, P., Soubrie, P., Le Fur, G., Maffrand, J. P., and Breliere, J. C. (1997) Biochemical and pharmacological activities of SR144190, a new potent non-peptide tachykinin NK2 receptor antagonist, *Neuropeptides 31*, 449−458.
16. Emonds-Alt, X., Golliot, F., Pointeau, P., Le Fur, G., and Breliere, J. C. (1993) Characterization of the binding sites of [^{3}H]SR48968, a potent nonpeptide radioligand antagonist of the neurokinin-2 receptor, *Biochem. Biophys. Res. Commun. 191*, 1172−1177.
17. Blaney, F. E., Raveglia, L. F., Artico, M., Cavagnera, S., Dartois, C., Farina, C., Grugni, M., Gagliardi, S., Luttmann, M. A., Martinelli, M., Nadler, G. M., Parini, C., Petrillo, P., Sarau, H. M., Scheideler, M. A., Hay, D. W. P., and Giardina, G. A. M. (2001) Stepwise modulation of neurokinin-3 and neurokinin-2 receptor affinity and selectivity in quinoline tachykinin receptor antagonists, *J. Med. Chem. 44*, 1675−1689.
18. Donnelly, D., Maudsley, S., Gent, J. P., Moser, R. M., Hurrell, C. R., and Findlay, J. B. C. (1999) Conserved polar residues in the transmembrane domain of the human tachykinin NK_2 receptor: functional roles and structural implications, *Biochem. J. 339*, 55−61.
19. Bhogal, N., Donnelly, D., and Findlay, J. B. C. (1994) The ligand binding site of the neurokinin 2 receptor, *J. Biol. Chem. 269*, 27269−27274.
20. Giolitti, A., Cucchi, P., Renzetti, A. R., Rotondaro, L., Zappitelli, S., and Maggi, C. A. (2000) Molecular determinants of peptide and non-peptide NK-2 receptor antagonists binding sites of the human tachykinin NK-2 receptor by site-directed mutagenesis, *Neuropharmacology 39*, 1422−1429.
21. Renzetti, A. R., Catalioto, R.-M., Criscuoli, M., Cucchi, P., Ferrer, C., Giolitti, A., Guelfi, M., Rotondaro, L., Warner, F. J., and Maggi, C. A. (1999) Relevance of aromatic residues in transmembrane segments V to VII for binding of peptide and nonpeptide antagonists to the human tachykinin NK_2 receptor, *J. Pharmacol. Exp. Ther. 290*, 487−495.
22. Renzetti, A. R., Catalioto, R.-M., Carloni, C., Criscuoli, M., Cucchi, P., Giolitti, A., Zappitelli, S., Rotondaro, L., and Maggi, C. A. (1999) Effects of Tyrosine-289-Phenylalanine mutation on binding and functional properties of the human tachykinin NK_2 receptor stably expressed in Chinese hamster ovary cells. *Biochem. Pharmacol. 57*, 899−906.
23. Holmgren, M., Lui, Y., Xu, Y., and Yellen, G. (1996) On the use of thiol-modifying agents to determine channel topology, *Neuropharmacology 35*, 797−804.
24. Boyd, N. D., Kage, R., Dumas, J. J., Krause, J. E., and Leeman, S. E. (1996) The peptide binding site of the substance P (NK-1) receptor localized by a photoreactive analogue of Substance P: Presence of a disulfide bond, *Proc. Natl. Acad. Sci. U.S.A. 93*, 433−437.
25. Haendler, B., Hechler, U., Becker, A., and Schleuning, W.-D. (1993) Extracellular cysteine residues 174 and 255 are essential for active expression of human endothelin receptor ET_B in *Escherichia coli*, *J. Cardiovasc. Pharmacol. 22*, S4−S6.
26. Nathans, J., Davenport, C. M., Maumenee, I. H., Lewis, R. L., Hejtmancik, J. F., Litt, M., Lovrian, E., Weleber, R., Bachynski, B., Zwas, F., Klingman, R., and Fishman, G. (1989) Molecular genetics of human blue cone monchromacy, *Science 245*, 831−838.
27. Teller, D. C., Okada, T., Behnke, C. A., Palczewski, K., and Stenkamp, R. E. (2001) Advances in determination of a high-resolution three-dimensional structure of rhodopsin, a model of G-protein-coupled receptors (GPCRs), *Biochemistry 40*, 7761−7772.
28. Yamano, Y., Ohyama, K., Chaki, S., Guo, D. F., and Inagami, T. (1992) Identification of amino acid residues of rat angiotensin II receptor for ligand binding by site directed mutagenesis, *Biochem. Biophys. Res. Commun. 187*, 1426−1431.

BI035475S